Supplementary material

This supplement is divided into five sections. Section 1 explains further details on the emission modelling methods. Section 2 describes how the maximum lifetime of CFC-113 was determined. Section 3 shows CFC-113a mixing ratios in air samples collected during the CARIBIC flights plotted against latitude and longitude. Section 4 shows and discusses CFC-113a mixing ratios from air samples collected during the Geophysica flights into the stratosphere in 2009-2010 and 2016 against CFC-11 mixing ratios. In Section 5 are the NAME footprints derived from 12-day backward simulations and showing the time integrated density of particles below 100 m altitude for the approximate times when samples were collected during the Taiwan campaigns at Hengchun in 2013 and 2015 and Cape Fuguei in 2014 and 2016.

1. Emission modelling methodology

The 2-D model extends from pole-to-pole and from the surface up to 24 km and has 288 grid boxes. The model was run for 84 years from 1934 to 2017. It begins in 1934 because that was considered early enough to be before emissions of CFC-113a and CFC-113 began. Using the corrections in Leedham-Elvidge et al. (accepted, ACP) we calculated the atmospheric lifetime of CFC-113a to be 51 years (30-148 years) based on an updated and improved mean age of air estimate. The atmospheric lifetime of CFC-113 is currently estimated to be 93 years with a 'likely' range of 82-109 years (Ko et al., 2013). The photolysis rates are calculated for each grid box as a function of seasonally varying temperature and the absorption spectra for the wavelengths 200–400 nm. For CFC-113a the absorption spectrum is taken from Davis et al. (2016) and for CFC-113 it is taken from Burkholder et al. (2015). For the reaction with $O(^1D)$ the rate coefficients used are 2.61 x 10^{-10} cm^3 molecule^{-1} s^{-1} and 2.33 x 10^{-10} cm^3 molecule^{-1} s^{-1} for CFC-113a and CFC-113 respectively (Baasandorj et al., 2011). The diffusive loss of gases out of the top of the model is controlled by making the mixing ratios immediately above the model a constant fraction (F) of the mixing ratios in the top layer of the model (22-24 km). Nearly all the loss of both compounds is above the model and so the atmospheric lifetimes are almost completely controlled by varying the F factor. The values of F were set to 0.6250 (0.0001-0.9854) for steady-state lifetimes of 51 years (30 years-148 years) for CFC-113a and to 0.8254 (0.7888-0.8618) for lifetimes of 93 years (82 years-109 years) for CFC-113. The minimum lifetime of 30 years for CFC-113a could not be achieved by adjusting the F value alone so was simulated by choosing a very small value for F of 0.0001 and by increasing the photolysis rate inside the model domain by a factor of 5.24. This is likely because the data used to determine the range (30-148 years) do not provide adequate constraint rather than implying that there may be unknown sinks.

The upper and lower emission uncertainties for CFC-113a and CFC-113 were determined by first calculating the uncertainty in matching the modelled mixing ratios with the observed mixing ratios using their recommended atmospheric lifetimes and secondly considering the uncertainty range in the lifetimes. In the first step the uncertainty is calculated from the square root of the sum of squares of the uncertainties in model transport, measurements and model fit, after which the calibration uncertainty was then added to this to give an overall uncertainty. The model transport uncertainty is assumed to be 5 % for both compounds based on the difference between observed mixing ratios of CFC-11 and CFC-12 at Cape Grim and those modelled (Reeves et al., 2005). As long-lived gases with reasonably well-known emissions and atmospheric mixing ratios this difference is taken to represent the uncertainty in the model transport. The average measurement uncertainty is the mean of the one sigma standard deviations derived as the square root of the sum of the squared uncertainties in sample repeats and repeated measurements of an air standard on the same day. This works out to be 0.8 % for CFC-113 and 3.9 % for CFC-113a. The model fit uncertainty is the mean percentage difference between the 'best fit' modelled mixing ratios and the observations which is 1.0 % for CFC-113 and 2.6 % for CFC-113a. Finally, the calibration uncertainty for CFC-113a is 3.8 % (Laube et al., 2014) and for CFC-113 is 0.5 % (Brad Hall, personal communication). This is the uncertainty in the NOAA calibration scale. We do not have the full calibration uncertainty for CFC-113 as the content of CFC-113a is currently unknown for the NOAA 'CFC-113' calibration as the two isomers are hard to separate from each other. Combining these uncertainties as described above gives overall uncertainties of ±5.7 % for CFC-113 and ±10.6 % for CFC-113a. The upper and lower bounds of the emissions were then estimated by re-running the model to fit the observed mixing ratios adjusted by these overall uncertainties. The upper bound is estimated using the lowest lifetime and the highest mixing ratios and the lower bound is estimated using the highest lifetime and the lowest mixing ratios.

2. Calculation of CFC-113 maximum lifetime

During the period 2003 onwards we calculate very small emissions for CFC-113 suggesting that the rate of change is dominated by its atmospheric lifetime. If we assume no sources of CFC-113, then we can calculate the lifetime of CFC-113 by using the change in its mixing ratios at Cape Grim and a rearrangement of the chemical continuity equation:

$$\tau = -\frac{\Delta t}{\ln\left(\frac{C_{t+\Delta t}}{C_t}\right)}$$

where τ is the lifetime, C_t is the mixing ratio at time t, and $C_{t+\Delta t}$ is the mixing ratio at time $t+\Delta t$ where Δt is the time interval between the two mixing ratios. By assuming that there are no sources, the lifetime calculated is the maximum value, since any source of CFC-113 would have to be balanced by a shorter lifetime. To account for the measurement variability, the lifetime was calculated five times using the annual mean observed mixing ratios separated by a running 10-year interval (i.e. 2003 to 2013, 2004 to 2014 etc up to 2007 to 2017). The resulting lifetime of 113 ± 4 years is then the mean $\pm$ the standard deviation of these five values. Accounting for the possible 2 % difference between the decay time and steady state lifetime gives an overall range of 113 ± 5 years.

3. CARIBIC flights

Figure S1a: CFC-113a mixing ratios from samples collected during CARIBIC aircraft campaign flights from 2009 to 2016 for each flight from Frankfurt, Germany (FRA) to Cape Town, South Africa (CPT) and Johannesburg, South Africa (JNB), with 1σ standard deviations as error bars.

Figure S1b: CFC-113a mixing ratios from samples collected over northern India during CARIBIC aircraft flights in 2013 going from Frankfurt, Germany (FRA) to Bangkok, Thailand, (BKK), with 1σ standard deviations as error bars.
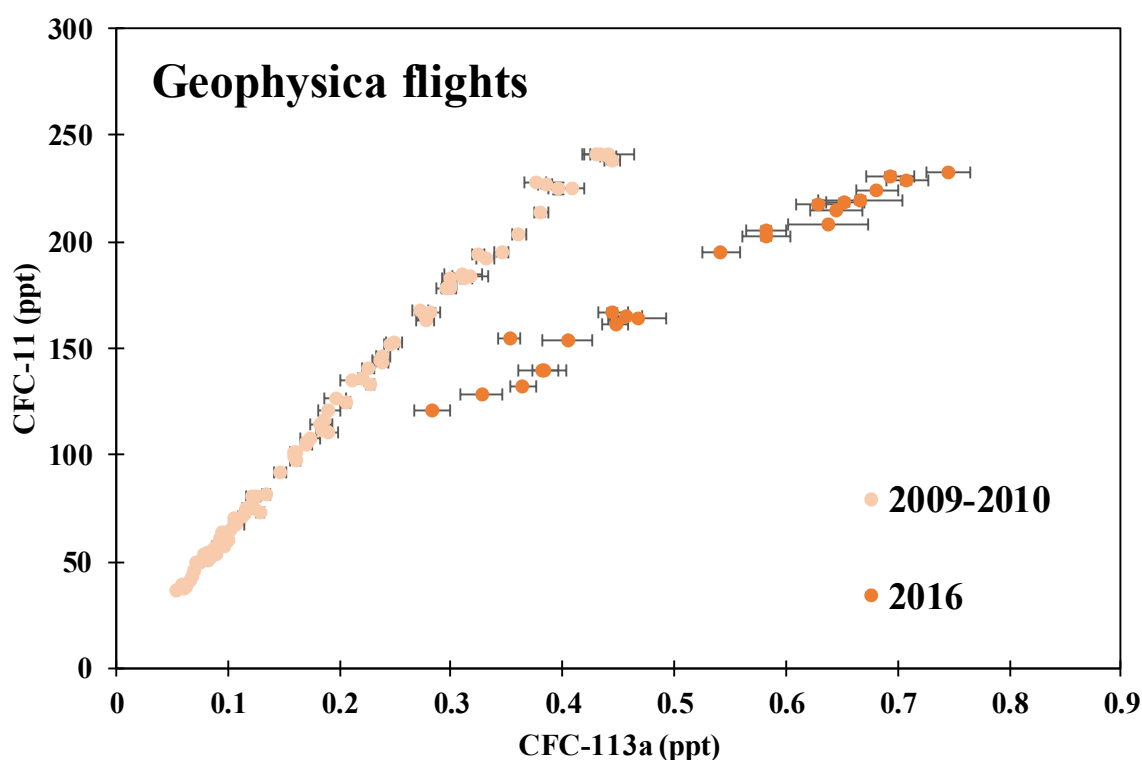
75   **4. Geophysica flights**

Figure S2: CFC-113a mixing ratios against CFC-11 mixing ratios from Geophysica research aircraft flights into the stratosphere in late 2009 and early 2010 published in Laube et al. (2014) and additional Geophysica research aircraft flights in 2016 in Kalamata (StratoClim project). The error bars represent the 1σ standard deviation.

80   Given that CFC-11 mixing ratios have declined over the last 25 years older air will have entered the stratosphere with higher mixing ratios, but will also have undergone more chemical processing. In addition, as the stratospheric lifetime of CFC-11 is shorter than its global lifetime, its mixing ratios will decline more rapidly in the stratosphere than in the troposphere. However, its vertical profile is a function of how its photolysis changes with altitude and

the rate of vertical transport. If photochemical loss were the main factor determining the vertical profile of both these CFCs, there would be a straight-line correlation, particularly since both have very similar lifetimes which should also lead to the intercept being very close to zero, which is seen for the 2009/10 flights (Figure S2). However, if the tropospheric trends of these CFCs are different then this can lead to curvature of the line. For example, as the tropospheric mixing ratio of CFC-11 is declining whilst it is increasing for CFC-113a, this should cause the line to curve towards higher CFC-113a mixing ratios which is apparent in the 2009/10 flights (Figure S2). Moreover, later profiles should have shallower gradients, which is what we see with the 2016 data compared to the 2009/10 data (Figure S2). The intercept for the 2016 data does not look like it will be near zero but if samples were collected at higher altitudes the data might curve closer towards zero (Figure S2). The Geophysica 2016 highest CFC-113a mixing ratio was 0.75 ± 0.02 ppt. The Tacolneston mixing ratio at this time was 0.72 ± 0.01 ppt. In 2009-2010 the Geophysica highest mixing ratio was 0.44 ± 0.01 ppt and at this time the Cape Grim mixing ratio was 0.43 ± 0.01 ppt. The highest mixing ratios observed in both campaigns agree quite well (within uncertainties) with tropospheric background mixing ratios at the time and can therefore be considered as representative of stratospheric entrance mixing ratios.

References not provided in the main manuscript:

Baasandorj, M., Feierabend, K. J. and Burkholder, J. B.: Rate Coefficients and ClO Radical Yields in the Reaction of O(^{1}D) with CClF$_2$CCl$_2$F, CCl$_3$CF$_3$, CClF$_2$CClF$_2$, and CCl$_2$FCF$_3$, Int. J. Chem. Kinet., 41(1987), 498–506, doi:10.1002/kin, 2011.
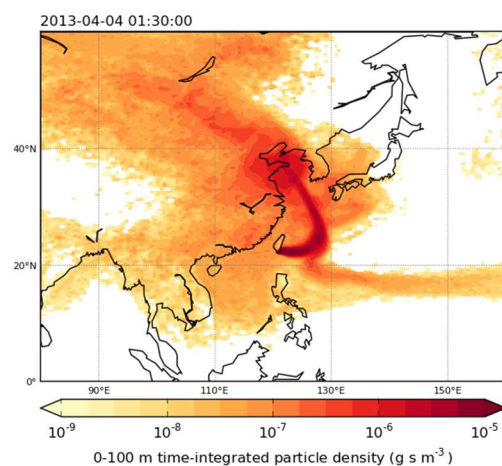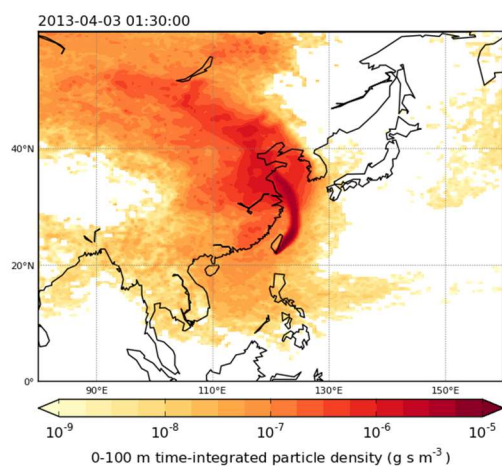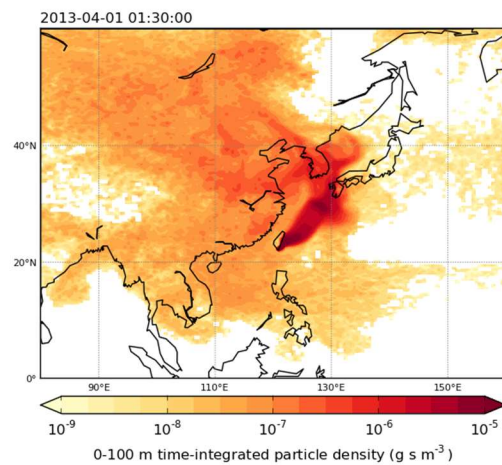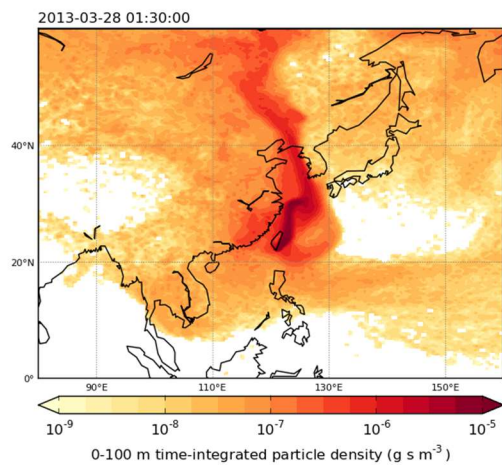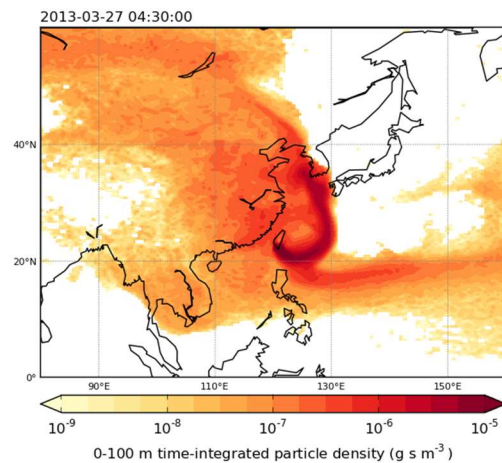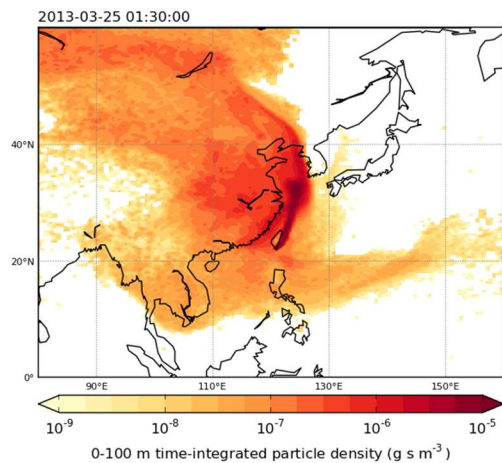
Burkholder, J. B., Sander, S. P., Abbatt, J. P. D., Barker, J. R., Huie, R. E., Kolb, C. E., Kurylo, M. J., Orkin, V. L., Wilmouth, D. M. and Wine, P. H.: Chemical Kinetics and Photochemical Data for Use in Atmospheric Studies Evaluation Number 18 NASA Panel for Data Evaluation. [online] Available from: https://jpldataeval.jpl.nasa.gov/pdf/JPL_Publication_15-10.pdf (Accessed 26 May 2017), 2015.
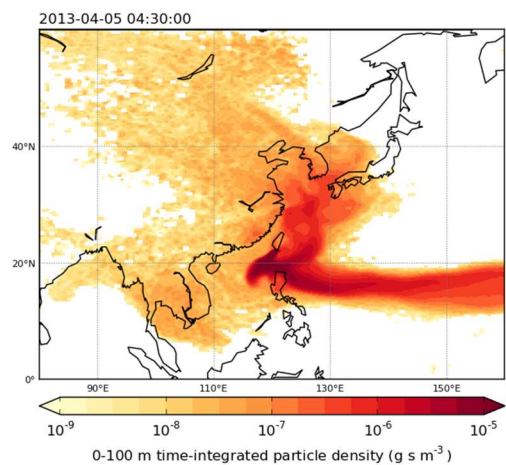
Davis, M. E., Bernard, F., McGillen, M. R., Fleming, E. L. and Burkholder, J. B.: UV and infrared absorption spectra, atmospheric lifetimes, and ozone depletion and global warming potentials for CCl$_2$FCCl$_2$F (CFC-112), CCl$_3$CClF$_2$ (CFC-112a), CCl$_3$CF$_3$ (CFC-113a), and CCl$_2$FCF$_3$ (CFC-114a), Atmos. Chem. Phys., 16(12), 8043–8052, doi:10.5194/acp-16-8043-2016, 2016.

5.1 NAME footprints for the Hengchun, Taiwan 2013 campaign

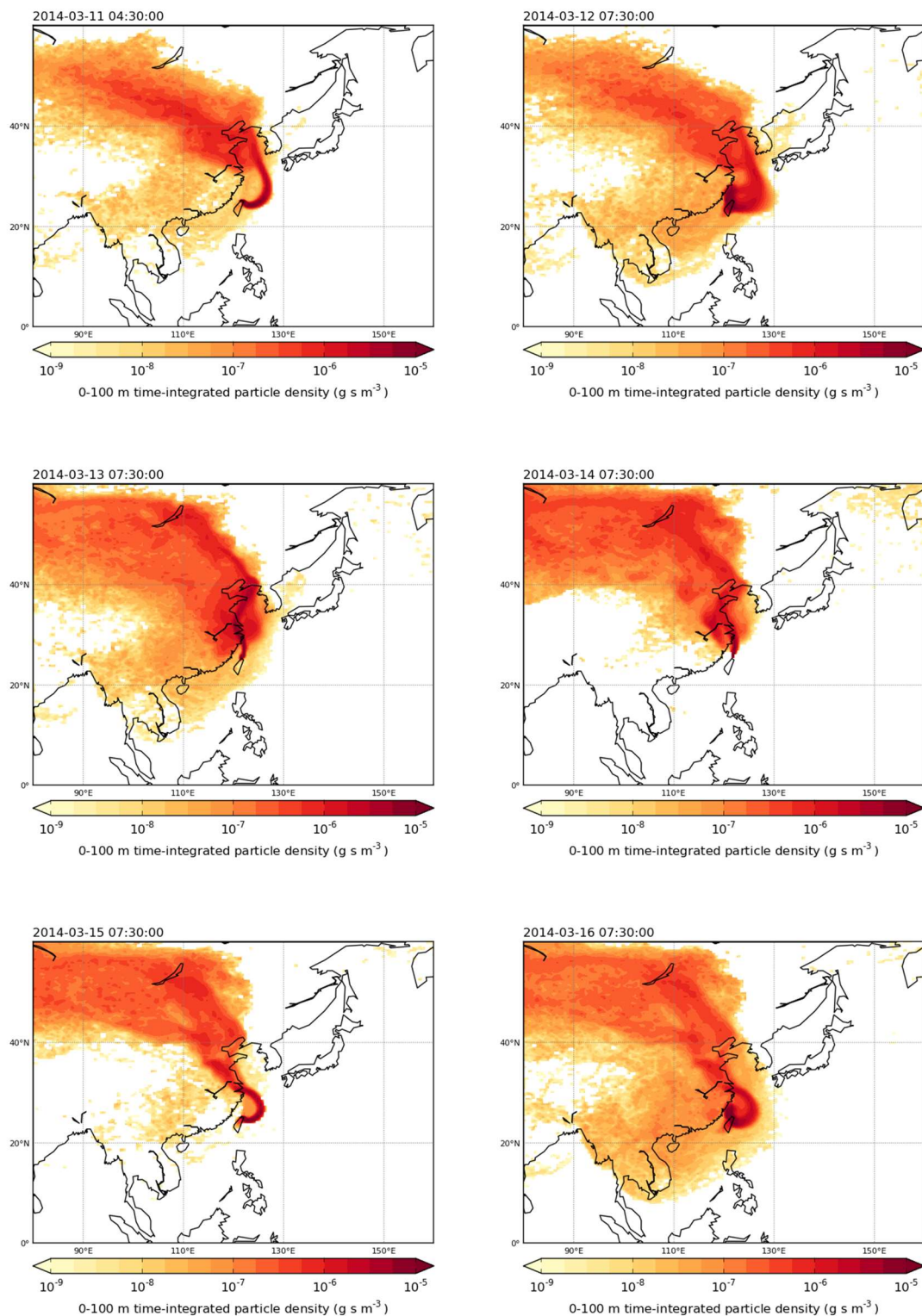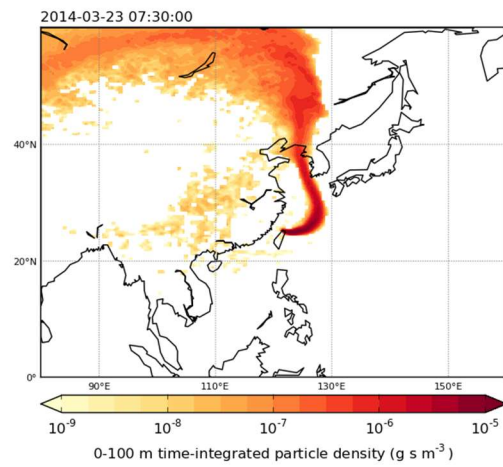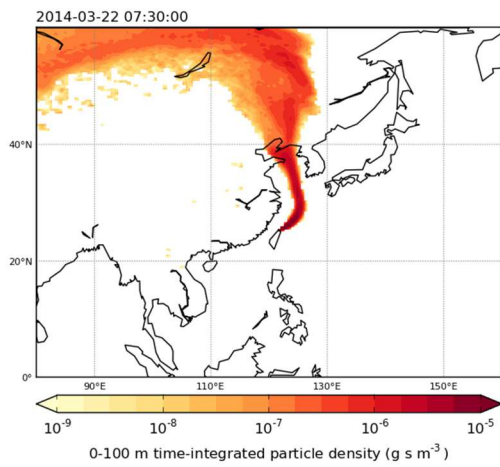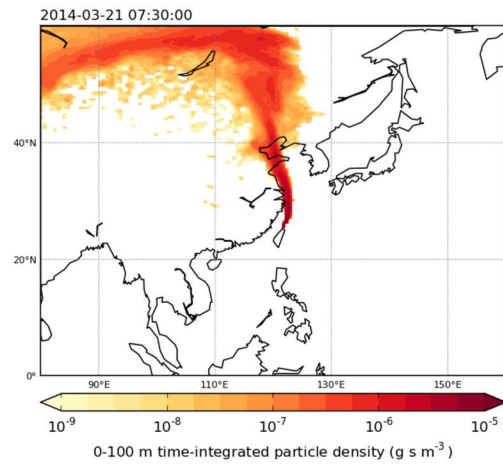
2013-03-07 04:30:00

0-100 m time-integrated particle density (g s m^{-3})

2013-03-08 04:30:00

0-100 m time-integrated particle density (g s m^{-3})

2013-03-11 04:30:00

0-100 m time-integrated particle density (g s m^{-3})

2013-03-12 01:30:00

0-100 m time-integrated particle density (g s m^{-3})

125

2013-03-13 01:30:00

0-100 m time-integrated particle density (g s m^{-3})

2013-03-14 01:30:00

0-100 m time-integrated particle density (g s m^{-3})

0-100 m time-integrated particle density (g s m⁻³)

2013-03-25 01:30:00

2013-03-27 04:30:00

0-100 m time-integrated particle density (g s m^{-3})

0-100 m time-integrated particle density (g s m^{-3})

130

2013-03-28 01:30:00

2013-04-01 01:30:00

0-100 m time-integrated particle density (g s m^{-3})

0-100 m time-integrated particle density (g s m^{-3})

2013-04-03 01:30:00

2013-04-04 01:30:00

0-100 m time-integrated particle density (g s m^{-3})

0-100 m time-integrated particle density (g s m^{-3})

2013-04-05 04:30:00

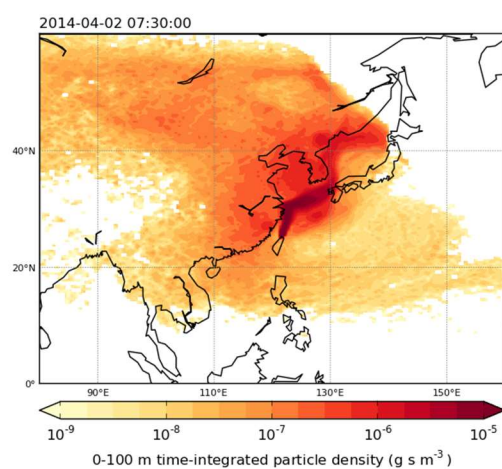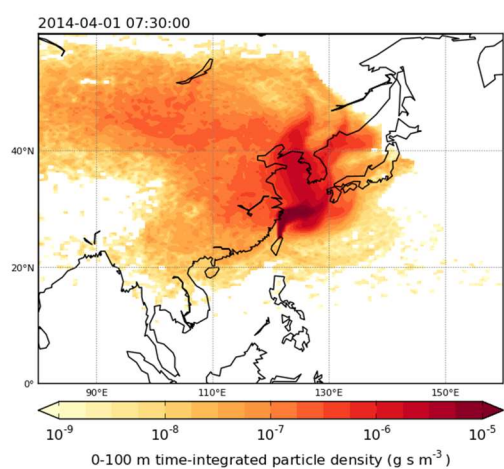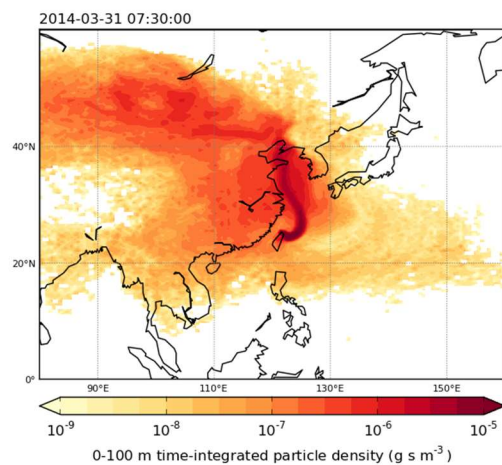0-100 m time-integrated particle density (g s m^{-3})

135

140

145

150

155

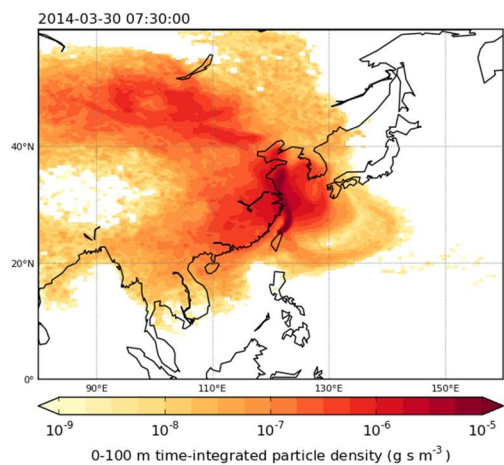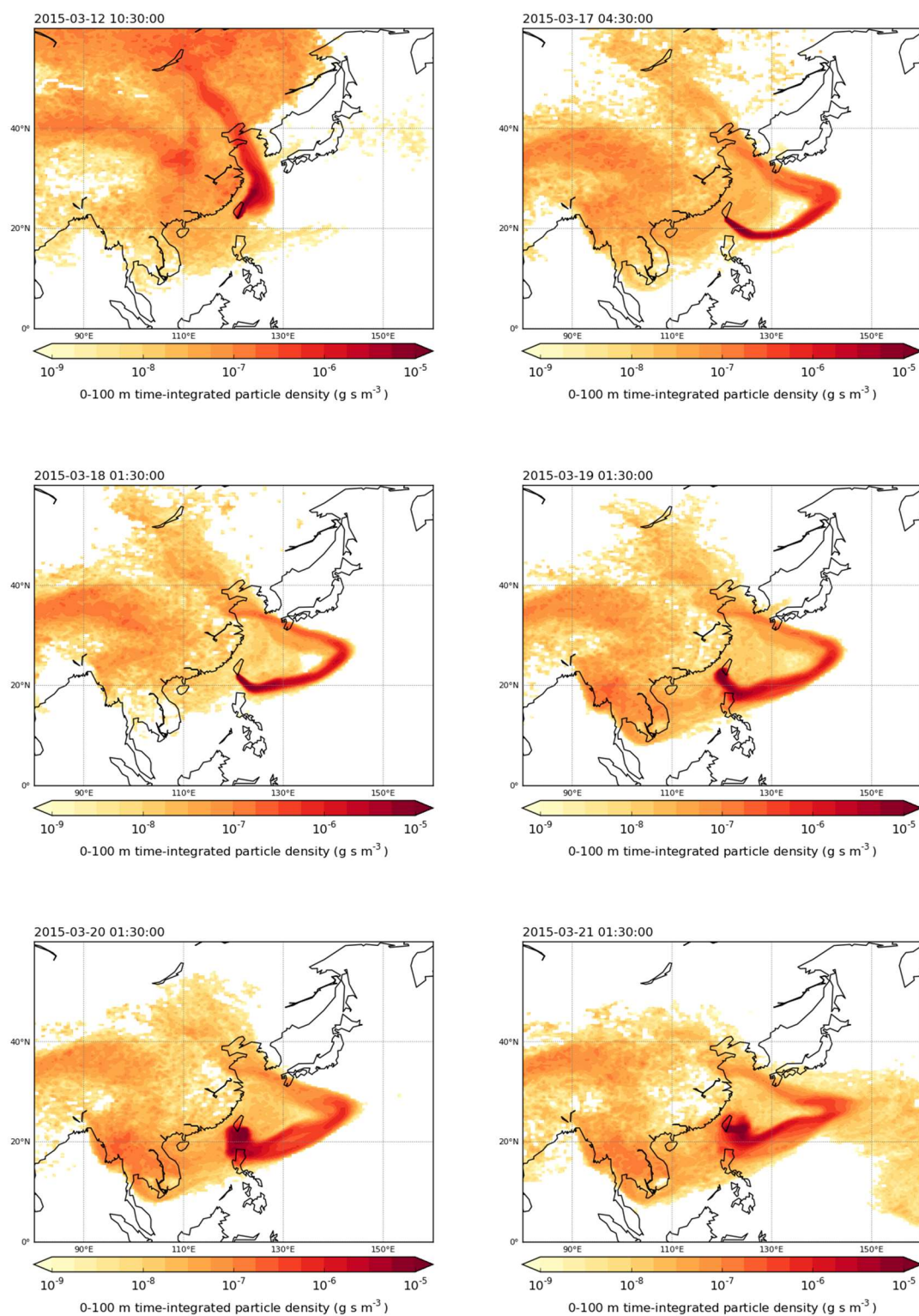## 5.2 NAME footprints for the Cape Fuguei, Taiwan 2014 campaign

160

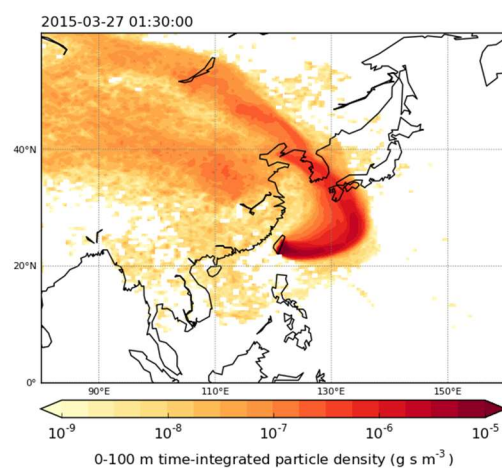2014-03-17 07:30:00

2014-03-18 07:30:00

0-100 m time-integrated particle density (g s m^{-3})

2014-03-19 07:30:00

2014-03-21 07:30:00

0-100 m time-integrated particle density (g s m^{-3})

2014-03-22 07:30:00

2014-03-23 07:30:00

0-100 m time-integrated particle density (g s m^{-3})

165

170

5.3 NAME footprints for the Hengchun, Taiwan 2015 campaign

180

2015-03-28 04:30:00

2015-03-29 01:30:00

0-100 m time-integrated particle density (g s m^{-3})

2015-03-30 01:30:00

2015-03-31 01:30:00

0-100 m time-integrated particle density (g s m^{-3})

2015-04-22 10:30:00

2015-04-23 01:30:00

0-100 m time-integrated particle density (g s m^{-3})

2015-04-23 10:30:00

0-100 m time-integrated particle density (g s m^{-3})

2015-04-24 01:30:00

0-100 m time-integrated particle density (g s m^{-3})

185

2015-04-24 10:30:00

0-100 m time-integrated particle density (g s m^{-3})

2015-04-25 01:30:00

0-100 m time-integrated particle density (g s m^{-3})

2015-04-25 10:30:00

0-100 m time-integrated particle density (g s m^{-3})

190

5.4 NAME footprints for the Cape Fuguei, Taiwan 2016 campaign

2016-03-16 09:30:00

0-100 m time-integrated particle density (g s m^{-3})

2016-03-20 04:30:00

0-100 m time-integrated particle density (g s m^{-3})

2016-03-21 06:00:00

0-100 m time-integrated particle density (g s m^{-3})

2016-03-24 05:00:00

0-100 m time-integrated particle density (g s m^{-3})

2016-03-24 06:30:00

0-100 m time-integrated particle density (g s m^{-3})

2016-03-25 04:30:00

0-100 m time-integrated particle density (g s m^{-3})

195

200

2016-04-12 06:30:00

2016-04-14 03:30:00

0-100 m time-integrated particle density (g s m^{-3})

2016-04-14 04:30:00

2016-04-14 07:00:00

0-100 m time-integrated particle density (g s m^{-3})

2016-04-15 02:30:00

2016-04-15 04:30:00

0-100 m time-integrated particle density (g s m^{-3})

2016-04-18 04:30:00

2016-04-19 04:00:00

0-100 m time-integrated particle density (g s m^{-3})

205

2016-04-25 04:30:00

2016-04-25 06:30:00

0-100 m time-integrated particle density (g s m^{-3})

2016-04-28 04:00:00

2016-04-28 06:00:00

0-100 m time-integrated particle density (g s m^{-3})

2016-04-29 02:30:00

0-100 m time-integrated particle density (g s m^{-3})

2016-04-29 04:30:00

0-100 m time-integrated particle density (g s m^{-3})

2016-04-29 06:00:00

0-100 m time-integrated particle density (g s m^{-3})